Original Article

Circ_0007099 upregulates GNG7 to function as a tumor inhibitor in gastric carcinoma by interacting with miR-425-3p

Zhipeng Zhang[1#], Yikai Zhou[1#], Na Zhou[2,3], Junda Yin[1], Xuechun Kuang[1,3]

[1]Department of Geratology Surgery, Xiangya Hospital, Central South University, Changsha, China; [2]Department of General Surgery, Xiangya Hospital, Central South University, Changsha, China; [3]Teaching and Research Section of Clinical Nursing, Xiangya Hospital, Central South University, Changsha, China

Contributions: (I) Conception and design: X Kuang, Z Zhang, Y Zhou; (II) Administrative support: X Kuang; (III) Provision of study materials or patients: Z Zhang, Y Zhou; (IV) Collection and assembly of data: N Zhou, J Yin; (V) Data analysis and interpretation: Z Zhang, Y Zhou; (VI) Manuscript writing: All authors; (VII) Final approval of manuscript: All authors.

[#]These authors contributed equally to this work.

Correspondence to: Xuechun Kuang. Department of Geratology Surgery, Xiangya Hospital, Central South University, 87 Xiangya Road, Kaifu District, Changsha 410008, China. Email: kxc1086@126.com.

Background: Circular RNAs (circRNAs) are usually dysregulated in human tumors and affect the malignant progression of tumors. Circ_0007099 is known to be downregulated in gastric carcinoma (GC), and this research was performed to investigate the regulatory function of circ_0007099 in GC progression.

Methods: The detection of circ_0007099, miR-425-3p, and G protein γ subunit 7 (GNG7) was performed via reverse transcription-quantitative polymerase chain reaction assay. Cell proliferation was determined by EdU and colony formation assays, and angiogenesis was assessed via a tube formation assay. Glucose metabolism was evaluated with commercial kits, and protein expression was measured by western blot. Dual-luciferase reporter and RNA immunoprecipitation assays were performed to validate the target interaction. An in vivo exploration of circ_0007099 was conducted using a xenograft tumor assay.

Results: Circ_0007099 was downregulated in GC patients and cells. Overexpression of circ_0007099 repressed cell proliferation, angiogenesis, and glucose metabolism while enhancing apoptosis in GC cells. Circ_0007099 exhibited a sponge effect on miR-425-3p, and the anti-tumor function of circ_0007099 was achieved by sponging miR-425-3p. Furthermore, miR-425-3p directly targeted GNG7, and miR-425-3p inhibition suppressed malignant progression by reducing GNG7 expression in GC cells. Circ_0007099 sponged miR-425-3p to upregulate the level of GNG7. We also found that *in vivo* tumor growth was reduced by circ_0007099 mediating the miR-425-3p/GNG7 axis.

Conclusions: This study demonstrated that circ_0007099 inhibits the malignant behavior of GC cells by binding to miR-425-3p, thus regulating the expression of GNG7.

Keywords: Circ_0007099; gastric cancer; miR-425-3p; GNG7

Submitted Jun 01, 2022. Accepted for publication Aug 15, 2022.
doi: 10.21037/jgo-22-684
View this article at: https://dx.doi.org/10.21037/jgo-22-684

Introduction

Gastric carcinoma (GC) is a multifactorial disease caused by multiple risk factors and is one of the most common causes of cancer-associated mortality worldwide (1). The early diagnosis rate is low in most countries with a high incidence of GC, and the overall therapeutic effect is poor for patients in advanced stages of the disease (2). There has been significant progress in the treatment of GC in recent years, especially with targeted therapy (3). Targeted molecules can improve diagnosis in the early stage and survival in advanced GC (4). Therefore, functional targets are essential in developing effective treatment strategies for GC.

Circular RNAs (circRNAs) are a novel type of RNA with unique closed-loop structures and exhibit a variety of biological roles in cancers (5). CircRNAs competitively interact with microRNAs (miRNAs) by acting as molecular sponges to regulate gene levels. The circRNA/miRNA/mRNA axis is one of the most common mechanisms in GC development (6). For instance, circ_0002570 accelerated cell invasion and tumor growth in GC by preventing miR-587–mediated VCAN gene degradation (7). Cui *et al.* revealed that circ_0006470 enhanced the migration and proliferation of GC cells by targeting the miR-27b-3p/PI3KCA axis (8).

Hsa_circ_0007099 is a less-studied circRNA derived from α/β hydrolase domain-containing protein 2 (ABHD2). An investigation of the global circRNA expression profile showed that circ_0007099 was downregulated in clinical GC samples (9). However, the regulatory function of circ_0007099 in GC has not been addressed. Li *et al.* discovered that miR-425-3p targeted ZC3H12A to accelerate malignant cell phenotypes in GC (10). G protein γ subunit 7 (GNG7) was shown to block GC cell metastasis, and circRNA CDR1as upregulated GNG7 levels to inhibit GC development by sponging miR-876-5p (11). Whether circ_0007099 can function as a natural sponge for miR-876-5p, thus affecting GNG7 expression in GC, remains to be explored.

Circ_0007099 was hypothesized to have a target relation with miR-425-3p, as well as miR-425-3p and GNG7. In addition, we aimed to analyze the circ_0007099 expression regulation for GNG7 by targeting miR-425-3p. The present study aimed to discover the functional molecular pathway of circ_0007099 in GC. We present the following article in accordance with the ARRIVE and MDAR reporting checklists (available at https://jgo.amegroups.com/article/view/10.21037/jgo-22-684/rc).

Methods

GC and normal tissues

Fifty-seven patients with GC who received surgical treatment at Xiangya Hospital of Central South University were included in the present study. GC tissues (n=57) and adjacent normal tissues (n=57) were collected after surgery, then conserved in liquid nitrogen for further experimentation. The procedures on the human samples were in accordance with the Declaration of Helsinki (as revised in 2013). All patients provided written informed consent, and this study was approved by the Ethics Committee of Xiangya Hospital of Central South University (No. 202112183).

Cell culture and transfection

GC cell lines (AGS and HGC-27) and a normal gastric epithelial cell line (GES-1) were purchased from BEINUO (Shanghai, China). Cell incubation with Dulbecco's modified eagle medium (DMEM; Hyclone, Logan, UT, USA), 10% fetal bovine serum (FBS; Gibco, Carlsbad, CA, USA), and 1% antibiotic solution (Gibco) was performed in a 5% CO_2 incubator at 37 ℃. The AGS and HGC-27 cells were cultured to 70% coverage, then transfected with plasmids and RNAs using a Lipofectamine™ 3000 Kit (Invitrogen, Carlsbad, CA, USA). The circ_0007099 sequence was cloned into a pCD5-ciR plasmid (GENESEED, Guangzhou, China) to construct a pCD5-ciR-circ_0007099 plasmid (circ_0007099). The mimic of miR-425-3p (miR-425-3p), mimic of negative control (miR-con), inhibitor of miR-425-3p (in-miR-425-3p), inhibitor of control (in-miR-con), small interfering (si) RNA of GNG7 (si-GNG7), and siRNA of control (si-con) were synthesized by RIBOBIO (Guangzhou, China).

Reverse transcription-quantitative polymerase chain reaction (RT-qPCR) assay

Tissue specimens and cell lysates were collected for total RNA extraction using a Trizol Kit (Solarbio, Beijing, China). Subsequently, a RevertAid First Strand cDNA Synthesis Kit and TaqMan One-Step RT-qPCR Kit (Solarbio) were used for reverse transcription and PCR detection according to the manufacturer's guidelines. Circ_0007099 and ABHD2 stabilities were assessed by RT-qPCR after total RNA treatment with 3 U/μg RNase R (GENESEED). The expression level was analyzed via the $2^{-\Delta\Delta Ct}$ method (12). The miRNA level was standardized by U6, while circRNA and mRNA were normalized to β-actin. The specific primers are shown in *Table 1*.

EdU assay

The proliferation detection was performed by an EdU Proliferation Kit (Sigma, St. Louis, MO, USA). In brief, cells were incubated with an EdU working solution, and the cell nuclei were stained with diamidinyl phenylindole (DAPI) in accordance with the user manuals. EdU^+ cells were counted as EdU and DAPI-merged cells under a

Table 1 Primers sequences used for RT-qPCR

Name	Primers for PCR (5'-3')
hsa_circ_0007099	Forward: GTTTGAACCTGAAGAGCCCC
	Reverse: TGTACAGTTGGGCCGGTCA
ABHD2	Forward: ATCACACGCAGCTTTTAGGT
	Reverse: GGAGTCTCCAGCATGGCATT
GNG7	Forward: CCCGAGCGCAGGGAG
	Reverse: CCCCGTTGTTCAGAGAGCTT
miR-425-3p	Forward: GTATGAATCGGGAATGTCGTGT
	Reverse: CTCAACTGGTGTCGTGGAG
β-actin	Forward: CTTCGCGGGCGACGAT
	Reverse: CCACATAGGAATCCTTCTGACC
U6	Forward: CTCGCTTCGGCAGCACA
	Reverse: AACGCTTCACGAATTTGCGT

RT-qPCR, reverse transcription-quantitative polymerase chain reaction.

fluorescence microscope (Olympus, Tokyo, Japan).

Colony formation assay

The AGS and HGC-27 cells were transplanted into 12-well plates with 200 cells in each well. The plates were incubated at 37 ℃ for 14 days, and then the cells were dyed with crystal violet (Sigma) for 20 min. The number of colonies formed was detected by Image J software (NIH, Bethesda, MD, USA).

Tube formation assay

The 96-well plates were coated with 60 μL Matrigel (BD Bioscience, San Diego, CA, USA), and the GC cells were co-cultured with 2×10^4 Human Umbilical Vein Endothelial Cells (HUVECs, BEINUO) for 48 h. Then, the capillary-like branches were counted under five random microscopic fields (×200).

Extracellular acidification rate (ECAR) assay

The ECAR assay was used to assess the glycolytic process. An XF96-well plate was inoculated with 2×10^4 AGS and HGC-27 cells for 18 h. An XF assay unbuffered medium containing 2 mM glutamine was used to replace the cell medium, followed by incubation with 10 mM glucose, 1 μM oligomycin, and 80 mM 2-deoxyglucose (2-DG). Afterward, the ECAR (mpH/min) was read by a Seahorse Extracellular Flux Analyzer XF96 (Seahorse Bioscience, Billerica, MA, USA).

Glucose consumption and lactate production

The cultured supernatant was collected for the evaluation of glycolysis. In accordance with the manufacturer's directions, the consumption of glucose and the production of lactate were examined with a Glucose Uptake Detection Kit and a Lactate Production Detection Kit (Sigma).

Western blot

A radioimmunoprecipitation (RIP) assay buffer (Sigma) was used for the protein extraction, followed by western blot detection with 50 μg of protein from each sample (13). The proteins were transferred to polyvinylidene fluoride (PVF) membranes (Sigma) and incubated with primary antibodies targeting Hexokinase II (HK2; Abcam, Cambridge, MA, USA; ab209847, 1:1,000), GNG7 (Sigma, SAB1410555, 1:1,000), and β-actin (Abcam, ab8227, 1:1,000) at 4 ℃ overnight. Then, the secondary antibody (ab205718, 1:5,000) was incubated at room temperature for 1 h. An ECL Substrate Kit (Abcam) visualized the protein bands in line with the manufacturer's protocol. Image J software (NIH) was used to analyze the protein levels.

Flow cytometry

Cells were collected at 72 h post-transfection, then apoptosis was evaluated by an Annexin V Detection Kit (Solarbio). Briefly, 5×10^5 AGS and HGC-27 cells were stained with10 μL of Annexin V-FITC and propidium iodide (PI) at 4 ℃ for 30 min. Apoptotic cells (Annexin V^+/PI^+ and Annexin V^+/PI^-) were examined with a flow cytometer (BD Biosciences), and the apoptosis rate (apoptotic cells/total cells) was calculated.

Dual-luciferase reporter assay

The circ_0007099 sequence was predicted to contain miR-425-3p binding sites, and wild-type (WT) luciferase plasmid circ_0007099-WT was constructed by molecular cloning into pmirGLO plasmid (Promega, Madison, WI, USA). Then the binding sites were mutated, and a mutant-type (MUT) plasmid circ_0007099-MUT was constructed

as a negative control. In addition, GNG7-3'UTR-WT and GNG7-3'UTR-MUT were used for the binding analysis between miR-425-3p and GNG7. Circ_0007099 or GNG7 3'UTR plasmid and miR-425-3p or miR-NC were co-transfected for 48 h, then the AGS and HGC-27 cells were collected for luciferase detection by a Dual-Luciferase Reporter Kit (Promega).

RNA immunoprecipitation (RIP) assay

The AGS and HGC-27 (2×10^6) cells were harvested, then a RIP assay was performed using an Imprint® RNA Immunoprecipitation Kit (Sigma) according to the manufacturer's instructions. Anti-immunoglobulin G (anti-IgG) was used as the control group for anti-Argonaute-2 (anti-Ago2). Total RNA was isolated from the magnetic beads. Circ_0007099, miR-425-3p, and GNG7 levels were measured by RT-qPCR.

Tumor xenograft assay

AGS mock (without transfection), pCD5-ciR, or circ_0007099 cells (2×10^6) were subcutaneously injected into BALB/c male nude mice (Vital River Laboratory Animal Technology Co. Ltd., Beijing, China). There were six mice in each group. Tumor growth was monitored every week, and tumor volume was calculated by length × width^2/2. After 4 weeks of injections, the tumors were dissected and weighed. The expression analysis of circ_0007099, miR-425-3p, and GNG7 was conducted with RT-qPCR and western blot. Additionally, the Ki67 protein level (Abcam, ab15580, 1:1,000) was examined via an immunohistochemistry (IHC) assay (14). All operating procedures abided by the Guide for the Care and Use of Laboratory Animals of NIH (National Institutes of Health, USA). This study was approved by the Animal Ethics Committee of Xiangya Hospital (No. CSU-2022-0906). A protocol was prepared before the study without registration.

Statistical analysis

A linear analysis was performed using Pearson's correlation coefficient. The experimental data were collected from three independent repeats and displayed as the mean ± standard deviation. The data were analyzed with SPSS 22.0 (SPSS Inc., Chicago, IL, USA). Statistical differences were detected by Student's *t*-test or analysis of variance (ANOVA) followed by Tukey's test, where $P<0.05$ was defined as a statistically significant difference.

Results

Circ_0007099 was downregulated in GC patients and cells

A heat-map analysis showed that many circRNAs were differentially expressed in GC tissues (*Figure 1A*), and circ_0007099 exhibited significant downregulation in GC samples (*Figure 1B*). Also, circ_0007099 was found to be downregulated in the 57 tumor tissues from GC patients relative to the adjacent normal tissues (*Figure 1C*). Furthermore, circ_0007099 levels were reduced in AGS and HGC-27 cells compared with GES-1 cells (*Figure 1D*). RT-qPCR data revealed that circ_0007099 expression was mostly unaffected by RNase R while ABHD2 was digested, suggesting that circ_0007099 was highly stable in GC cells (*Figure 1E,1F*). The abnormal expression level of circ_0007099 implied its potential role in GC progression.

Circ_0007099 reduced proliferation, angiogenesis, and glucose metabolism but induced apoptosis in GC cells

The biological function of circ_0007099 was analyzed after transfection of pCD5-ciR or circ_0007099. The RT-qPCR results indicated that circ_0007099 levels were increased by about 4-fold in circ_0007099-transfected cells relative to pCD5-ciR-transfected cells (*Figure 2A*). EdU$^+$ cells in the EdU assay (*Figure 2B,2C*) and cell colonies in the colony formation assay (*Figure 2D,2E*) demonstrated that the cell proliferation ability of the circ_0007099 group was repressed compared with the pCD5-ciR group. The tube formation assay showed that angiogenesis was suppressed by overexpression of circ_0007099 in the AGS and HGC-27 cells (*Figure 2F,2G*). The upregulation of circ_0007099 resulted in inhibitory effects on ECAR (*Figure 2H,2I*), glucose consumption (*Figure 2J*), and lactate production (*Figure 2K*), which suggested that circ_0007099 blocked glucose metabolism in GC cells. Moreover, HK2 protein expression was downregulated by circ_0007099 transfection in the AGS and HGC-27 cells (*Figure 2L,2M*). After circ_0007099 was overexpressed, flow cytometry revealed that the apoptotic rate was significantly elevated (*Figure 2N,2O*). The above evidence identified that circ_0007099 impeded cell development in GC.

Circ_0007099 acted as a miR-425-3p sponge

Compared with the control groups, miR-425-3p was highly

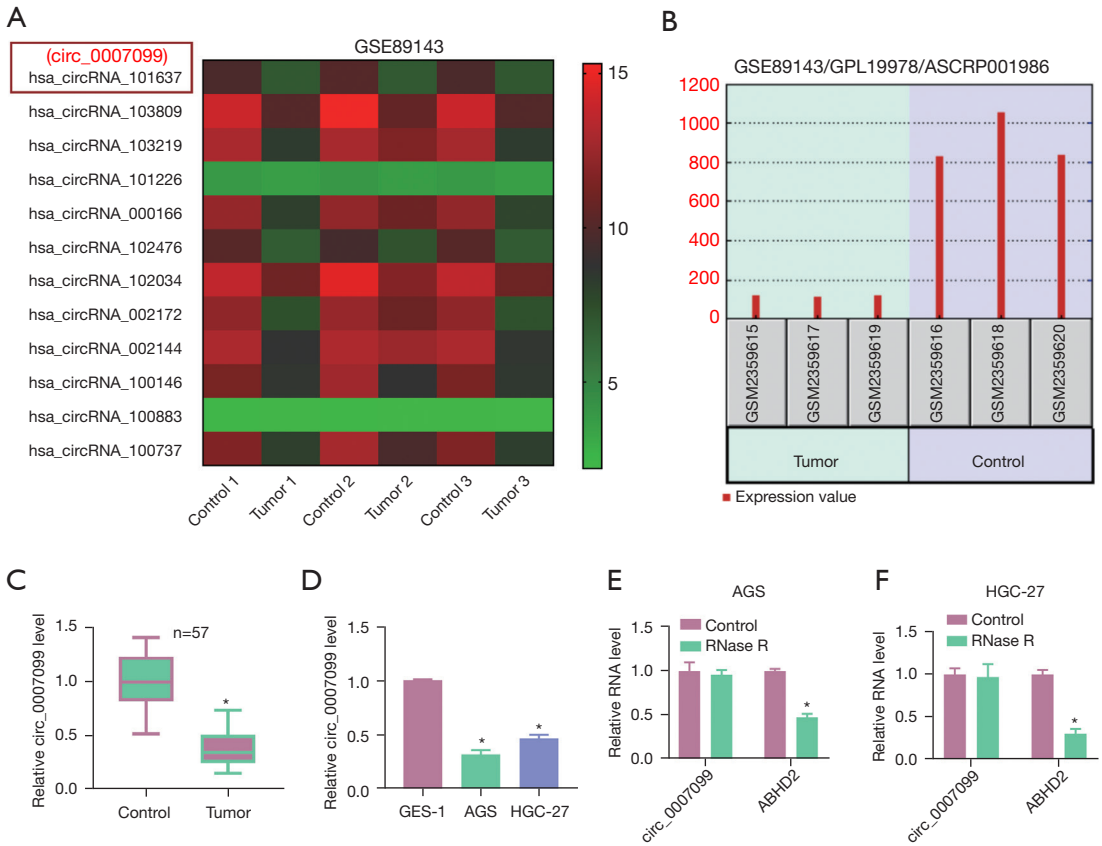

Figure 1 Circ_0007099 is downregulated in GC patients and cells. (A) Dysregulated circRNAs in GC tissues in the GSE89143 dataset. (B) Circ_0007099 downregulation in GC tissues in GSE89143. (C,D) RT-qPCR assay shows circ_0007099 levels in 57 GC samples (C) and AGS/HGC-27 cells (D), as well as normal controls and GES-1 cells. (E,F) Circ_0007099 and ABHD2 levels examined by RT-qPCR after RNA treatment with RNase R. *, P<0.05. GC, gastric carcinoma; RT-qPCR, reverse transcription-quantitative polymerase chain reaction.

expressed in GC tissues (*Figure 3A*), and circ_0007099 exhibited a negative relation (r=–0.8319, P<0.0001) with miR-425-3p in 57 GC samples (*Figure 3B*). RT-qPCR also indicated that miR-425-3p levels were higher in AGS and HGC-27 cells than in GES-1 cells (*Figure 3C*). More interestingly, miR-425-3p expression was downregulated by circ_0007099 overexpression in AGS and HGC-27 cells (*Figure 3D*). The binding sites between the circ_0007099 and miR-425-3p sequences were revealed by Targetscan website, as shown in *Figure 3E*. The dual-luciferase reporter assay demonstrated that miR-425-3p upregulation induced luciferase signal inhibition of the circ_0007099-WT group but not the circ_0007099-MUT group in AGS and HGC-27 cells (*Figure 3F,3G*). In addition, high levels of circ_0007099 and miR-425-3p were found in the anti-Ago2 group relative to the anti-IgG group in the RIP assay (*Figure 3H,3I*). Therefore, circ_0007099 served as a miR-425-3p sponge.

Circ_0007099 induced an anti-tumor response in GC cells by absorbing miR-425-3p

The effect of miR-425-3p on the function of circ_0007099 was researched. Transfection of miR-425-3p clearly upregulated the level of miR-425-3p in AGS and HGC-27 cells compared with the miR-con transfection group (*Figure 4A,4B*). Additionally, circ_0007099-mediated miR-425-3p downregulation was reversed following the introduction of miR-425-3p (*Figure 4C,4D*). The inhibiting influence of circ_0007099 on cell proliferation (*Figure 4E-4H*) and tube formation ability (*Figure 4I,4J*) was counteracted by the miR-425-3p mimic. ECAR

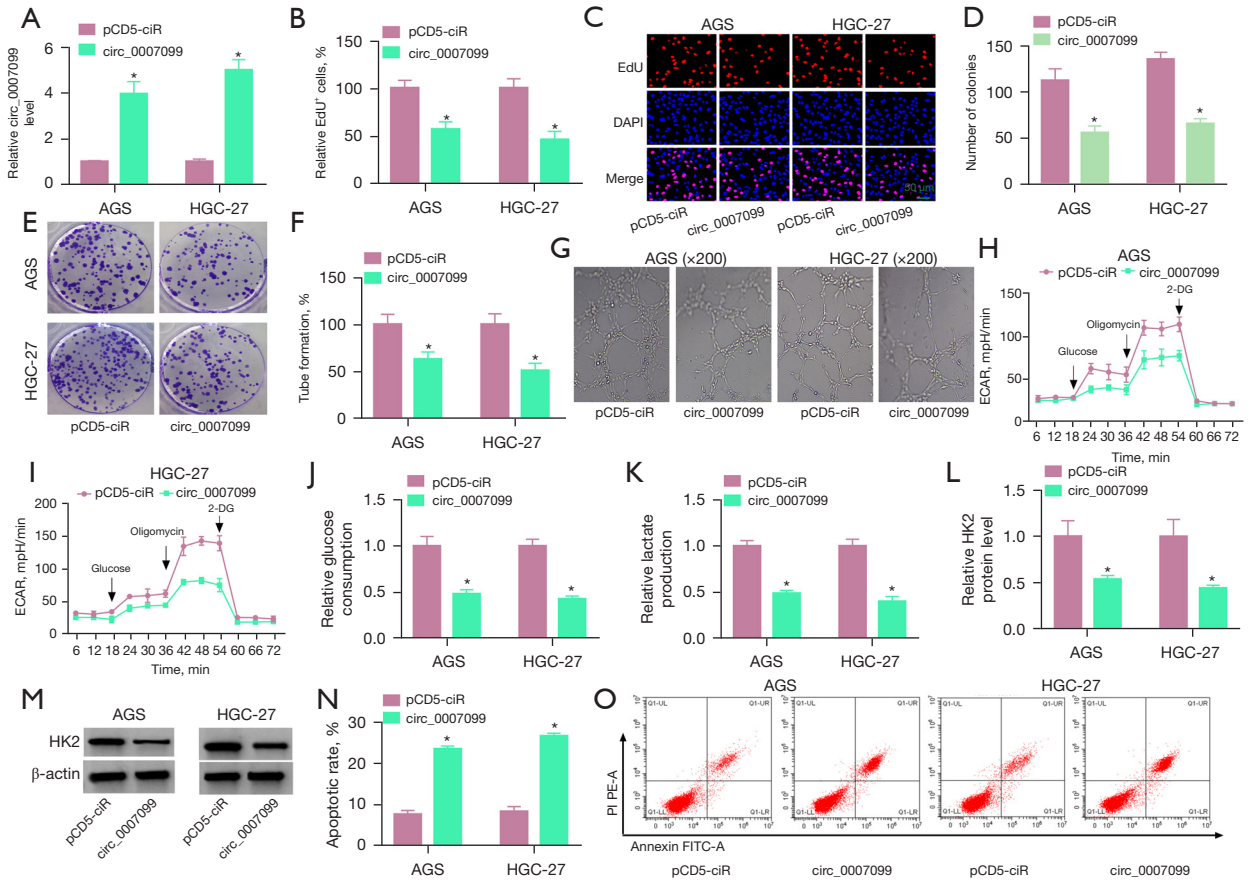

Figure 2 Circ_0007099 reduces proliferation, angiogenesis, and glucose metabolism but induces apoptosis in GC cells. AGS and HGC-27 cells are transfected with pCD5-ciR and circ_0007099, respectively. (A) RT-qPCR analysis of circ_0007099 levels. The RT-qPCR results indicate that circ_0007099 levels are increased by about 4-fold in circ_0007099-transfected cells relative to pCD5-ciR-transfected cells. (B-E) EdU assay (B,C) and colony formation assay (D,E) results of proliferation detection. (B,C) EdU+ cells in the EdU assay demonstrate that the cell proliferation ability of the circ_0007099 group is repressed compared with the pCD5-ciR group. (D,E) The cells are dyed with crystal violet (Sigma) for 20 min. The number of colonies formed is detected by Image J software. The figures reveal circ_0007099 can inhibit the proliferation of GC cells compared with transfecting with pCD5-ciR. Magnification: 100×. (F,G) The tube formation assay assessment of angiogenetic ability. The capillary-like branches are counted under five random microscopic fields. The tube formation assay show that angiogenesis is suppressed by overexpression of circ_0007099 in the AGS and HGC-27 cells. Magnification: 200×. (H-K) ECAR (H,I), glucose consumption (J), and lactate production (K) are detected for evaluation of glucose metabolism. The upregulation of circ_0007099 results in inhibitory effects on ECAR (H,I), glucose consumption (J), and lactate production (K), which suggest that circ_0007099 blocks glucose metabolism in GC cells. (L,M) Western blot shows the protein determination of HK2. HK2 protein expression is downregulated by circ_0007099 transfection in the AGS and HGC-27 cells. (N,O) Flow cytometry analysis of cell apoptosis. The results reveal that the apoptotic rate is significantly elevated after circ_0007099 is overexpressed. *, P<0.05. ECAR, extracellular acidification rate; GC, gastric carcinoma; RT-qPCR, reverse transcription-quantitative polymerase chain reaction.

(*Figure 4K,4L*), glucose consumption (*Figure 4M,4N*), lactate production (*Figure 4O,4P*), and HK2 protein expression (*Figure 4Q,4R*) revealed that miR-425-3p overexpression abolished circ_0007099-induced inhibition of the glycolytic process in AGS and HGC-27 cells. Also, the apoptotic rate was reduced in the circ_0007099 + miR-425-3p group compared with the circ_0007099 + miR-con group (*Figure 4S,4T*). These results confirmed that the tumor-inhibitory effect of circ_0007099 was due to sponging miR-425-3p in GC.

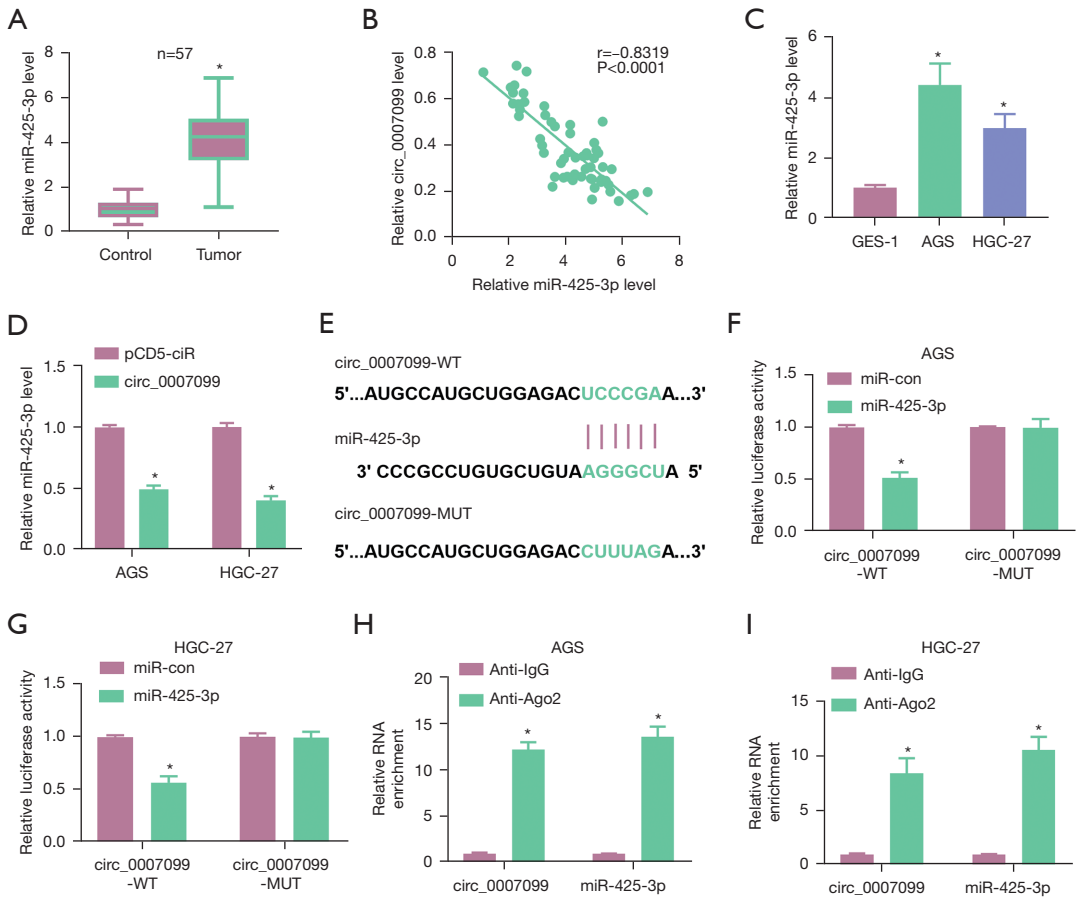

Figure 3 Circ_0007099 acts as a miR-425-3p sponge. (A) The miR-425-3p quantification conducted by RT-qPCR in GC and normal tissues. (B) The linear relation between circ_0007099 and miR-425-3p analyzed by Pearson's correlation coefficient. (C) The miR-425-3p expression measured via RT-qPCR in GC and normal cells. (D) Overexpression efficiency of circ_0007099 assessed by RT-qPCR. (E) The binding sites between circ_0007099 and miR-425-3p predicted by Targetscan. (F-I) The target binding between circ_0007099 and miR-425-3p analyzed by dual-luciferase reporter assay (F,G) and RIP assay (H,I). *, P<0.05. WT, wild-type; MUT, mutant-type; GC, gastric carcinoma; RT-qPCR, reverse transcription-quantitative polymerase chain reaction.

GNG7 was identified as a target gene of miR-425-3p

RT-qPCR revealed that GNG7 mRNA levels were decreased in GC tissue samples relative to normal controls (*Figure 5A*). Pearson's correlation coefficient indicated that miR-425-3p was negatively associated with GNG7 in the GC samples (r=–0.7834, P<0.0001) (*Figure 5B*). The protein detection by western blot showed that GNG7 was downregulated in GC tissues (*Figure 5C*) and AGS/HGC-27 cells (*Figure 5D*) compared with normal tissues and cells. The inhibitory efficiency of in-miR-425-3p was significant in AGS and HGC-27 cells compared with the in-miR-con group (*Figure 5E*). Inhibition of miR-425-3p promoted GNG7 protein levels in AGS and HGC-27 cells (*Figure 5F*). The binding sites between miR-425-3p and GNG7 using Targetscan are shown in *Figure 5G*. The luciferase activity was inhibited after co-transfection with miR-425-3p and GNG7-3'UTR-WT, while no conspicuous change was noticed after co-transfection with miR-425-3p and GNG7-3'UTR-MUT (*Figure 5H,5I*). The RIP assay further confirmed that miR-425-3p combined with GNG7 in AGS and HGC-27 cells (*Figure 5J,5K*). GNG7 was directly downregulated by miR-425-3p.

Downregulation of miR-425-3p inhibited the malignant behavior of GC cells by upregulating GNG7

GNG7 protein expression was knocked down by si-

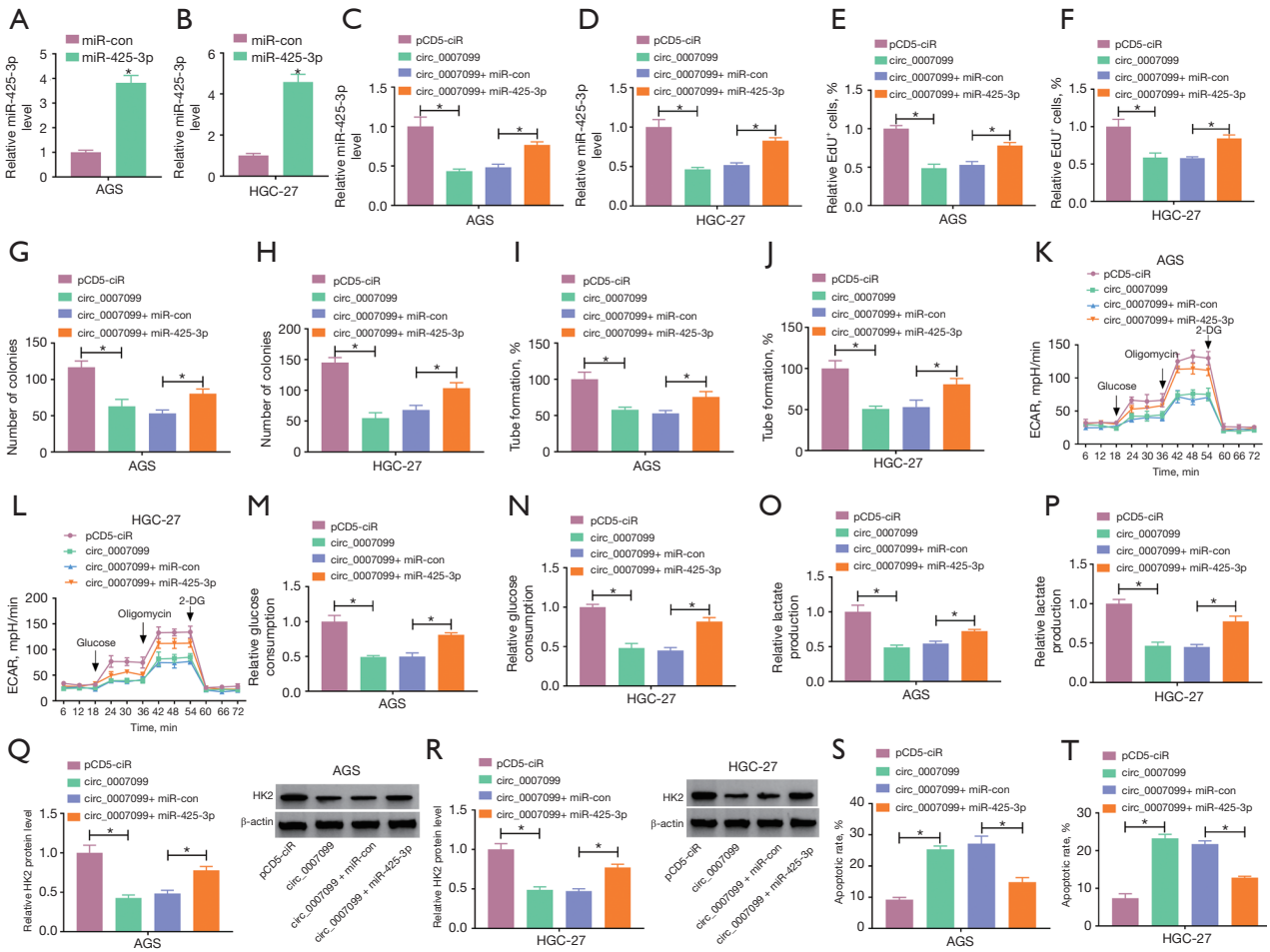

Figure 4 Circ_0007099 induces an anti-tumor response in GC cells by absorbing miR-425-3p. (A,B) miR-425-3p quantified by RT-qPCR after transfection with miR-con or miR-425-3p. (C-T) AGS and HGC-27 cells transfected with pCD5-ciR, circ_0007099, circ_0007099 + miR-con, or circ_0007099 + miR-425-3p. (C,D) miR-425-3p levels identified by RT-qPCR. (E-H) Cell proliferation assessment using EdU (E,F) and colony formation (G,H) assays. (I,J) Angiogenesis identified by the tube formation assay. (K-P) Glycolysis evaluation using detection kits for ECAR (K,L), glucose consumption (M,N), and lactate production (O,P). (Q,R) HK2 protein levels identified by western blot. (S,T) Cell apoptosis analysis using flow cytometry. *, P<0.05. GC, gastric carcinoma; RT-qPCR, reverse transcription-quantitative polymerase chain reaction.

GNG7 in AGS and HGC-27 cells, in contrast to the si-NC group (*Figure 6A,6B*). In addition, si-GNG7 attenuated the promoting effect of in-miR-425-3p on GNG7 protein levels (*Figure 6C,6D*). The EdU assay (*Figure 6E,6F*) and colony formation assay (*Figure 6G,6H*) demonstrated that miR-425-3p inhibitor reduced cell proliferation, which was partially abrogated by si-GNG7. The tube formation assay revealed that in-miR-425-3p-induced suppression of angiogenesis was restored after knockdown of GNG7 (*Figure 6I,6J*). Downregulation of miR-425-3p inhibited ECAR (*Figure 6K,6L*), glucose consumption (*Figure 6M,6N*), lactate production (*Figure 6O,6P*), and HK2 protein levels (*Figure 6Q,6R*) by elevating the expression of GNG7 in AGS and HGC-27 cells. Flow cytometry demonstrated that silencing GNG7 decreased the apoptosis promotion caused by in-miR-425-3p (*Figure 6S,6T*). Thus, miR-425-3p regulated GC progression by targeting GNG7.

Circ_0007099 upregulated GNG7 expression by sponging miR-425-3p

Using Pearson's correlation coefficient analysis, we found

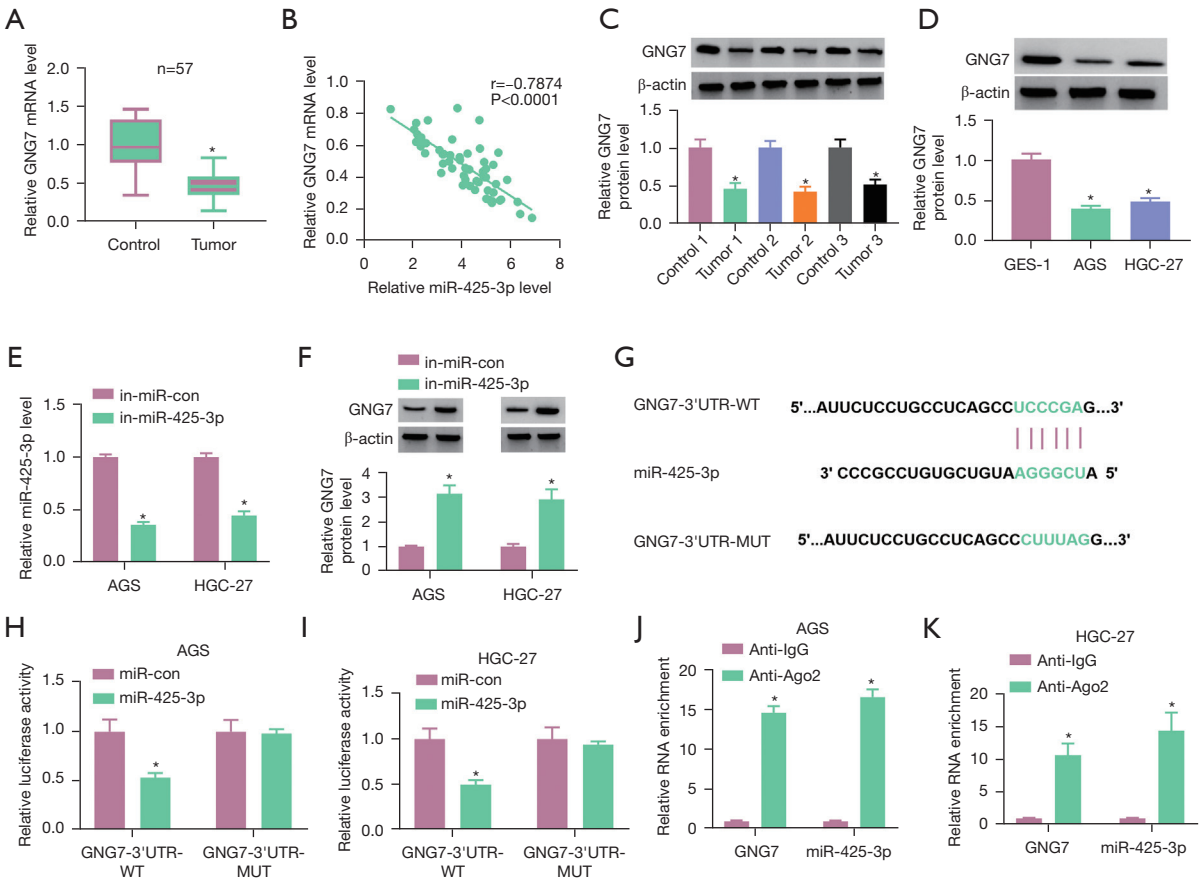

Figure 5 GNG7 is identified as a target gene of miR-425-3p. (A) The GNG7 mRNA expression determined by RT-qPCR in GC samples. (B) Pearson's correlation coefficient analysis of the linear relation between miR-425-3p and GNG7. (C,D) Western blot determines the GNG7 protein expression in GC tissues (C) and cells (D). (E,F) RT-qPCR and western blot results of the transfection efficacy of in-miR-425-3p. (G) Targetscan indicates the binding sites between miR-425-3p and GNG7. (H-K) Dual-luciferase reporter assay (H,I) and RIP assay (J,K) results of the interaction between GNG7 and miR-425-3p in AGS and HGC-27 cells. *, P<0.05. WT, wild-type; MUT, mutant-type; GC, gastric carcinoma; RT-qPCR, reverse transcription-quantitative polymerase chain reaction.

a positive relationship (r=0.6795, P<0.0001) between the expression levels of circ_0007099 and GNG7 in GC tissues (*Figure 7A*). The western blot assay revealed that circ_0007099 increased the protein level of GNG7, but miR-425-3p transfection counterbalanced this regulation in AGS and HGC-27 cells (*Figure 7B,7C*). Taken together, these results indicated that circ_0007099 regulated GNG7 levels by sequestering miR-425-3p.

Circ_0007099 reduced tumor growth in vivo by regulating miR-425-3p and GNG7 levels

The xenograft tumor assay in mice showed that tumor volume (*Figure 8A*) and weight (*Figure 8B*) were significantly inhibited in the circ_0007099 group relative to the pCD5-ciR and mock groups. The tumor images are shown in *Figure 8C*. Circ_0007099 levels were enhanced in the tumor tissues of the circ_0007099 group in contrast to the mock and pCD5-ciR groups (*Figure 8D*). Overexpression of circ_0007099 induced miR-425-3p downregulation (*Figure 8E*) and GNG7 protein upregulation (*Figure 8F*) in tumor tissues. The IHC assay indicated that Ki67 protein expression in mice was reduced by circ_0007099 (*Figure 8G*). In summary, circ_0007099 inhibited tumorigenesis *in vivo* by targeting the miR-425-3p/GNG7 axis.

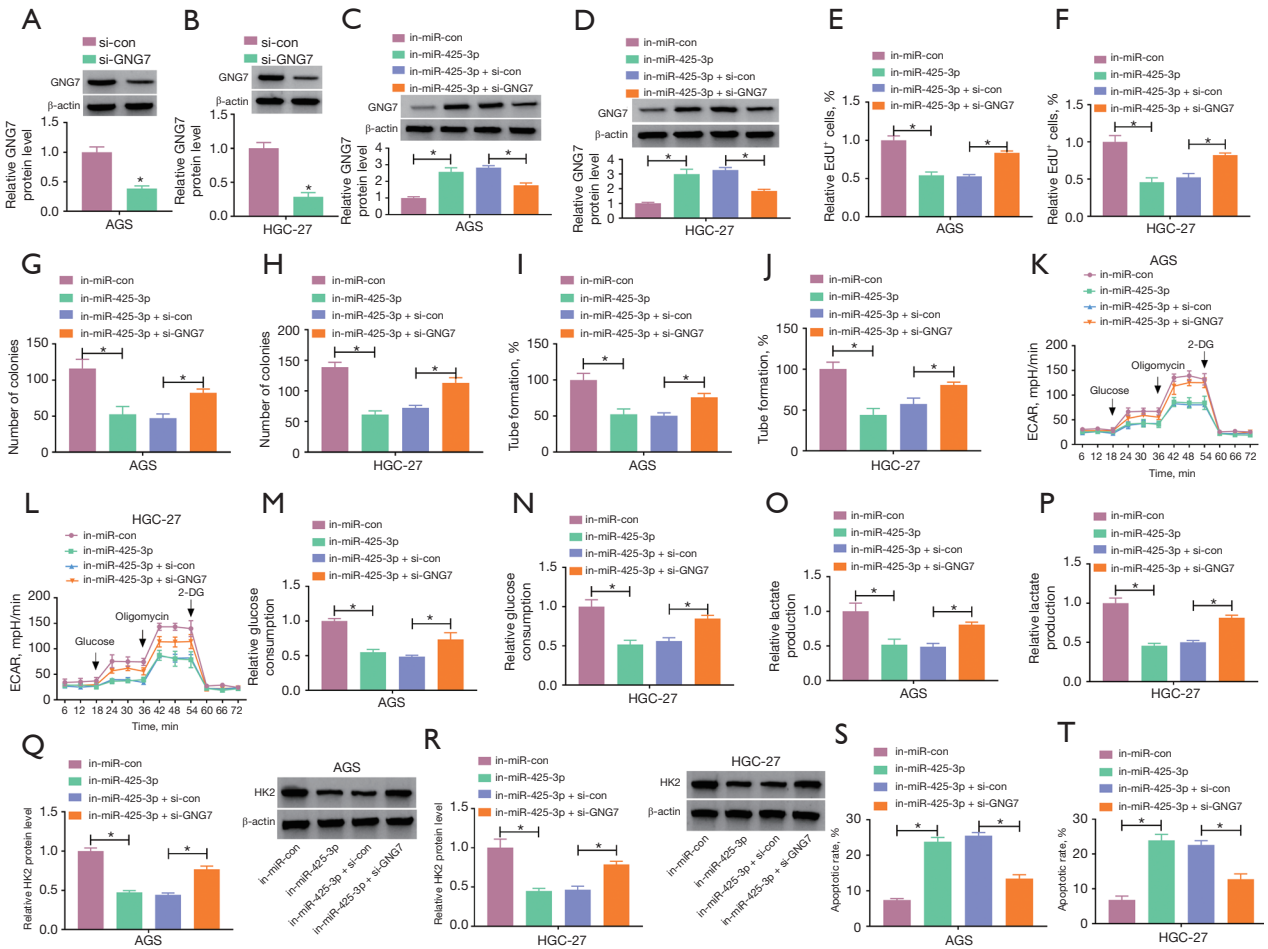

Figure 6 Downregulation of miR-425-3p inhibits the malignant behaviors of GC cells by upregulating GNG7. (A,B) GNG7 protein levels examined by western blot in AGS and HGC-27 cells transfected with si-con or si-GNG7. (C-T) AGS and HGC-27 cells transfected with in-miR-con, in-miR-425-3p, in-miR-425-3p + si-con, or in-miR-425-3p + si-GNG7. (C,D) Western blot measures the protein expression of GNG7. (E-H) EdU assay (E,F) and colony formation assay (G,H) analysis of cell proliferation. (I,J) Tube formation assay results of tube formation ability. (K-P) Glycolysis detection performed by ECAR (K,L), glucose consumption (M-N), and lactate production (O,P). (Q,R) The protein analysis of HK2 using western blot. (S,T) Cell apoptosis assessed by flow cytometry. *, P<0.05. GC, gastric carcinoma.

Discussion

Shao *et al.* reported that circ_0007099 was a downregulated circRNA in human GC tissues (9). Consistent with this abnormal expression pattern, circ_0007099 was conspicuously reduced in our GC tissue samples and cell lines. More importantly, our data validated that circ_0007099 functioned as a tumor inhibitor in GC by increasing GNG7 expression via miR-425-3p sponging.

CircRNAs have multiple biological properties, including widespread expression, tissue/cell-specificity, and high stability to resist RNase R digestion (15). In addition to the aberrant downregulation in GC, we found that circ_0007099 was stable and showed high resistance to RNase R in GC cells. A growing body of evidence has demonstrated that dysregulated circRNAs serve as oncogenic factors or anti-tumor molecules in GC. For example, circ-ARHGAP26 was shown to reduce cell apoptosis and promote cell proliferation in GC cells (16), Hsa-circ-000684 contributed to GC cell migration and tube formation abilities *in vitro* (17), Hsa_circ_0000993 exhibited inhibitory regulation of proliferation and motility in GC cells (18), and hsa_circ_0001368 impeded cell development to act as a tumor repressor in

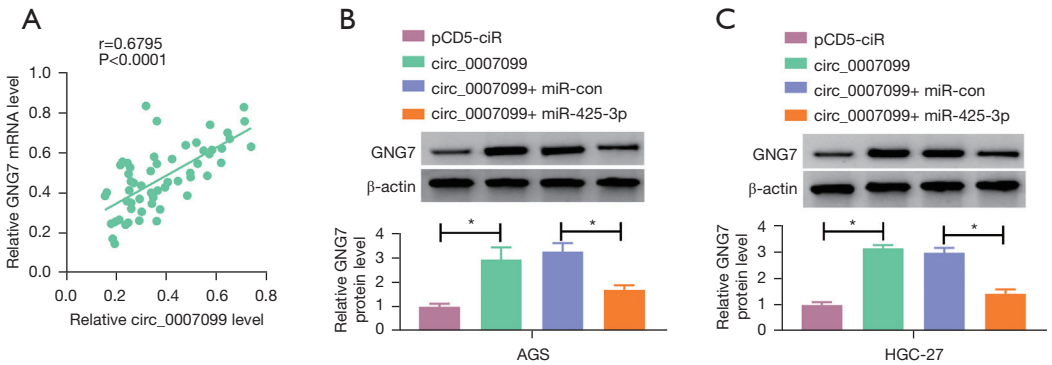

Figure 7 Circ_0007099 upregulates GNG7 expression via sponging miR-425-3p. (A) The relationship between circ_0007099 and GNG7 analyzed by Pearson's correlation coefficient. (B,C) GNG7 protein analysis conducted by western blot after transfection with pCD5-ciR, circ_0007099, circ_0007099 + miR-con, or circ_0007099 + miR-425-3p. *, P<0.05.

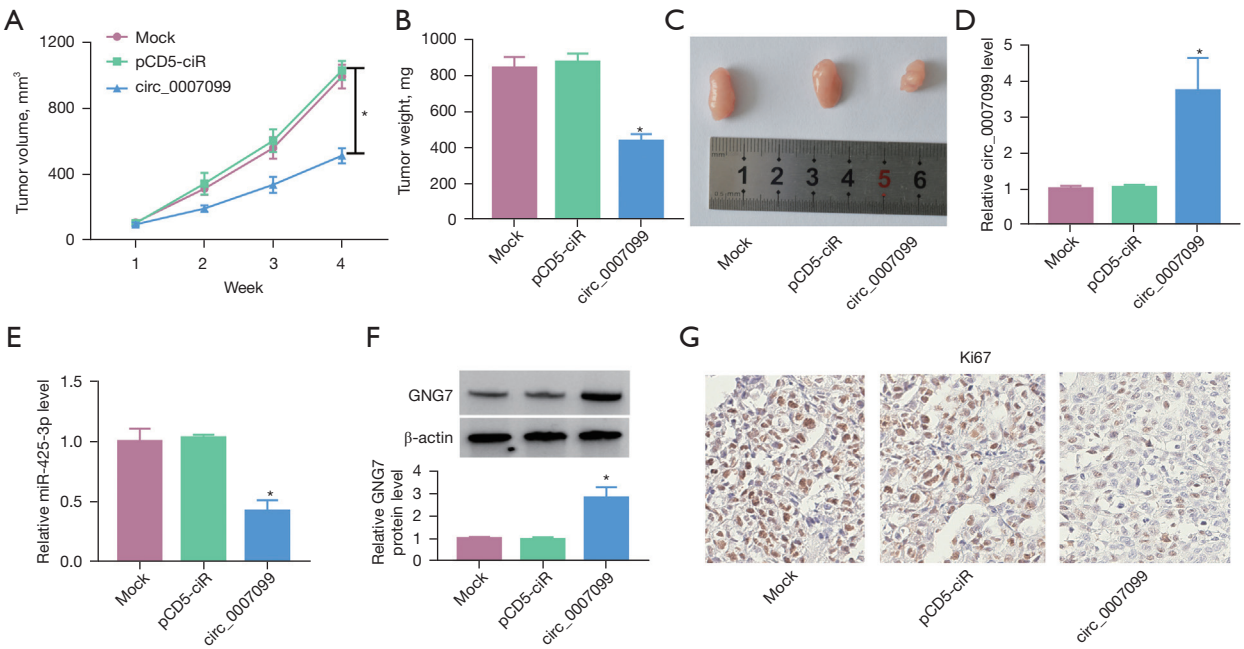

Figure 8 Circ_0007099 reduces tumor growth *in vivo* by regulating miR-425-3p and GNG7 levels. A tumor xenograft model of the mock, pCD5-ciR, or circ_0007099 mouse groups. (A,B) Tumor volume (A) and weight (B) measurements (C) Tumor images of each group. (D,E) Circ_0007099 (D) and miR-425-3p (E) levels assessed by RT-qPCR. (F,G) GNG7 (F) and Ki67 (G) protein levels examined by western blot and IHC assay (200×), respectively. *, P<0.05. RT-qPCR, reverse transcription-quantitative polymerase chain reaction.

GC (19). In this study, overexpression of circ_0007099 caused inhibition of angiogenesis and proliferation but apoptosis promotion in GC cells. Additionally, glycolytic indicators showed that glycolysis metabolism was suppressed by circ_0007099 in GC cells. Glycolysis has been found to support cancer progression (20,21), and noncoding RNAs are key regulators of the glycolytic pathway (22). Thus, our finding that circ_0007099 regulated glycolysis also confirmed that circ_0007099 repressed the malignant development of GC cells.

The miRNA sponge effects of circRNAs have been revealed in previous reports of GC. For example, circRNA_104433 accelerated tumor growth by inactivating miR-497-5p in GC (23), and circHIAT1 suppressed epithelial-

mesenchymal transition via miR-21 downregulation (24). Lai *et al.* reported that circRNA0047905 worked as a sponge for miR-1227-5p and miR-4516, initiating and promoting the progression of GC (25). In this study, miR-425-3p was verified as a miRNA target for circ_0007099, and the tumor-inhibiting influence of circ_0007099 on GC cellular processes was attenuated by miR-425-3p. At least in part, circ_0007099 inhibited GC development by sponging miR-425-3p.

G protein γ subunit 7 (GNG7), a member of the Gγ family, has been reported to be downregulated in multiple cancers. Decreased GNG7 expression was associated with hypermethylation of the GNG7 promoter region or decreased Zeste homolog 2 enhancer (EZH2) and increased disabling homolog 2 interacting protein (DAB2IP). In addition, most studies have shown that GNG7 was a potential tumor suppressor. In esophageal cancer, tumors with high GNG7 expression were less aggressive than those with low GNG7 expression *in vitro* and *in vivo*. In clear cell renal cell carcinoma, cells with lower levels of GNG7 showed an increased G2/M cell cycle phase. In gastrointestinal tumors, GNG7 inhibited cell growth *in vitro* and *in vivo* by upregulating the expression of the cyclin-dependent kinase inhibitor $p27^{Kip1}$. In addition, GNG7 was the first reported Gγ protein involved in autophagy. GNG7 induced autophagy and cell death by inhibiting the MTOR pathway and inhibits cell division by regulating the actin cytoskeleton. In this study, we found the expression of GNG7 was downregulated in GC tissue samples and cell lines, consistent with previous studies.

Furthermore, the miRNA/mRNA axis has been shown to be involved in the pathogenesis of GC. GC malignant progression was retarded by miR-146b-5p and miR-339-5p targeting TRAF6 and ALKBH1, respectively (26,27). In addition, miR-194 and miR-103a-3p contributed to proliferation and migration capacities by controlling the expression of SUFU and ATF7, respectively (28,29). Our results identified the target relationship between miR-425-3p and GNG7. Furthermore, downregulation of miR-425-3p repressed the malignant behavior of GC cells by upregulating GNG7. Thus, miR-425-3p acted as an oncogenic RNA by targeting GNG7 in GC. Circ_0007099 induced the upregulation of GNG7 by sponging miR-425-3p in GC cells, suggesting that circ_0007099 was implicated in GC progression via the miR-425-3p/GNG7 axis. Our *in vivo* data also confirmed that tumor growth in mice was reduced by the circ_0007099/miR-425-3p/GNG7 network.

CircRNAs have pivotal diagnostic values and therapeutic possibilities for GC. Wei *et al.* reported that circRNA_102958 was overexpressed in GC and may be a potential biomarker for diagnosis (30). Huang *et al.* stated that circ_0000745 was downregulated in GC and could serve as a diagnostic target for GC (31). Similarly, the abnormal level of circ_0007099 in our study implied that circ_0007099 might be a biological molecule for GC diagnosis. The anti-tumor effect of circ_0007099 also suggested that circ_0007099 could be a molecular marker for GC treatment. The further identification needs to be performed in the clinical exploration.

Conclusions

In conclusion, circ_0007099 inhibited the regulation of GC malignant behaviors by reducing miR-425-3p to elevate GNG7 expression levels. The circ_0007099/miR-425-3p/GNG7 axis plays a vital role in the progression of GC.

Acknowledgments

Funding: The study was funded by The Natural Science Foundation of Hunan Province of China (grant No. 2020JJ4885).

Footnote

Reporting Checklist: The authors have completed the ARRIVE and MDAR reporting checklists. Available at https://jgo.amegroups.com/article/view/10.21037/jgo-22-684/rc

Data Sharing Statement: Available at https://jgo.amegroups.com/article/view/10.21037/jgo-22-684/dss

Conflicts of Interest: All authors have completed the ICMJE uniform disclosure form (available at https://jgo.amegroups.com/article/view/10.21037/jgo-22-684/coif). The authors have no conflicts of interest to declare.

Ethical Statement: The authors are accountable for all aspects of the work in ensuring that questions related to the accuracy or integrity of any part of the work are appropriately investigated and resolved. The procedures on the human samples were in accordance with the Declaration of Helsinki (as revised in 2013). All patients provided written informed consent, and this study was approved by the Ethics Committee of Xiangya Hospital of Central South University (No. 202112183). All operating procedures

abided by the Guide for the Care and Use of Laboratory Animals of NIH (National Institutes of Health, USA). This study was approved by the Animal Ethics Committee of Xiangya Hospital (No. CSU-2022-0906).

References

1. Lyons K, Le LC, Pham YT, et al. Gastric cancer: epidemiology, biology, and prevention: a mini review. Eur J Cancer Prev 2019;28:397-412.
2. Jiang L, Gong X, Liao W, et al. Molecular targeted treatment and drug delivery system for gastric cancer. J Cancer Res Clin Oncol 2021;147:973-86.
3. Joshi SS, Badgwell BD. Current treatment and recent progress in gastric cancer. CA Cancer J Clin 2021;71:264-79.
4. Patel TH, Cecchini M. Targeted Therapies in Advanced Gastric Cancer. Curr Treat Options Oncol 2020;21:70.
5. Wang X, Li H, Lu Y, et al. Circular RNAs in Human Cancer. Front Oncol 2020;10:577118.
6. Ruan Y, Li Z, Shen Y, et al. Functions of circular RNAs and their potential applications in gastric cancer. Expert Rev Gastroenterol Hepatol 2020;14:85-92.
7. Yang L, Zhou YN, Zeng MM, et al. Circular RNA Circ-0002570 Accelerates Cancer Progression by Regulating VCAN via MiR-587 in Gastric Cancer. Front Oncol 2021;11:733745.
8. Cui Y, Cao J, Huang S, et al. circRNA_0006470 promotes the proliferation and migration of gastric cancer cells by functioning as a sponge of miR-27b-3p. Neoplasma 2021;68:1245-56.
9. Shao Y, Li J, Lu R, et al. Global circular RNA expression profile of human gastric cancer and its clinical significance. Cancer Med 2017;6:1173-80.
10. Li H, Zhao C, Zhao H, et al. Elevated linc00936 or silenced microRNA-425-3p inhibits immune escape of gastric cancer cells via elevation of ZC3H12A. Int Immunopharmacol 2021;95:107559.
11. Jiang J, Li R, Wang J, et al. Circular RNA CDR1as Inhibits the Metastasis of Gastric Cancer through Targeting miR-876-5p/GNG7 Axis. Gastroenterol Res Pract 2021;2021:5583029.
12. Livak KJ, Schmittgen TD. Analysis of relative gene expression data using real-time quantitative PCR and the 2(-Delta Delta C(T)) Method. Methods 2001;25:402-8.
13. Zhong JX, Kong YY, Luo RG, et al. Circular RNA circ-ERBB2 promotes HER2-positive breast cancer progression and metastasis via sponging miR-136-5p and miR-198. J Transl Med 2021;19:455.
14. Sun J, Xin K, Leng C, et al. Down-regulation of SNHG16 alleviates the acute lung injury in sepsis rats through miR-128-3p/HMGB3 axis. BMC Pulm Med 2021;21:191.
15. Cai H, Li Y, Niringiyumukiza JD, et al. Circular RNA involvement in aging: An emerging player with great potential. Mech Ageing Dev 2019;178:16-24.
16. Wangxia LV, Fang Y, Liu Y, et al. Circular RNA ARHGAP26 is over-expressed and its downregulation inhibits cell proliferation and promotes cell apoptosis in gastric cancer cells. Saudi J Gastroenterol 2019;25:119-25.
17. Lin S, Song S, Sun R, et al. Oncogenic circular RNA Hsa-circ-000684 interacts with microRNA-186 to upregulate ZEB1 in gastric cancer. FASEB J 2020;34:8187-203.
18. Zhong S, Wang J, Hou J, et al. Circular RNA hsa_circ_0000993 inhibits metastasis of gastric cancer cells. Epigenomics 2018;10:1301-13.
19. Lu J, Zhang PY, Li P, et al. Circular RNA hsa_circ_0001368 suppresses the progression of gastric cancer by regulating miR-6506-5p/FOXO3 axis. Biochem Biophys Res Commun 2019;512:29-33.
20. Ganapathy-Kanniappan S. Molecular intricacies of aerobic glycolysis in cancer: current insights into the classic metabolic phenotype. Crit Rev Biochem Mol Biol 2018;53:667-82.
21. Abbaszadeh Z, Çeşmeli S, Biray Avcı Ç. Crucial players in glycolysis: Cancer progress. Gene 2020;726:144158.
22. Li T, Xian HC, Dai L, et al. Tip of the Iceberg: Roles of CircRNAs in Cancer Glycolysis. Onco Targets Ther 2021;14:2379-95.
23. Wei W, Mo X, Yan L, et al. Circular RNA Profiling Reveals That circRNA_104433 Regulates Cell Growth by Targeting miR-497-5p in Gastric Cancer. Cancer Manag Res 2020;12:15-30.
24. Quan J, Dong D, Lun Y, et al. Circular RNA circHIAT1 inhibits proliferation and epithelial-mesenchymal transition of gastric cancer cell lines through downregulation of miR-21. J Biochem Mol Toxicol

2020;34:e22458.
25. Lai Z, Yang Y, Wang C, et al. Circular RNA 0047905 acts as a sponge for microRNA4516 and microRNA1227-5p, initiating gastric cancer progression. Cell Cycle 2019;18:1560-72.
26. Ding JN, Zang YF, Ding YL. MiRNA-146b-5p inhibits the malignant progression of gastric cancer by targeting TRAF6. Eur Rev Med Pharmacol Sci 2020;24:8837-44.
27. Wang C, Huang Y, Zhang J, et al. MiRNA-339-5p suppresses the malignant development of gastric cancer via targeting ALKBH1. Exp Mol Pathol 2020;115:104449.
28. Peng Y, Zhang X, Ma Q, et al. MiRNA-194 activates the Wnt/β-catenin signaling pathway in gastric cancer by targeting the negative Wnt regulator, SUFU. Cancer Lett 2017;385:117-27.
29. Hu X, Miao J, Zhang M, et al. miRNA-103a-3p Promotes Human Gastric Cancer Cell Proliferation by Targeting and Suppressing ATF7 in vitro. Mol Cells 2018;41:390-400.
30. Wei J, Wei W, Xu H, et al. Circular RNA hsa_circRNA_102958 may serve as a diagnostic marker for gastric cancer. Cancer Biomark 2020;27:139-45.
31. Huang M, He YR, Liang LC, et al. Circular RNA hsa_circ_0000745 may serve as a diagnostic marker for gastric cancer. World J Gastroenterol 2017;23:6330-8.

(English Language Editor: D. Fitzgerald)

Cite this article as: Zhang Z, Zhou Y, Zhou N, Yin J, Kuang X. Circ_0007099 upregulates GNG7 to function as a tumor inhibitor in gastric carcinoma by interacting with miR-425-3p. J Gastrointest Oncol 2022;13(4):1626-1639. doi: 10.21037/jgo-22-684

